

## Electrochemical Behavior of Al-Si Alloy in Phosphoric Acid Containing Halogen or Oxyhalogen Anions

A. A. Ghoneim<sup>\*</sup>, M. A. Ameer and A.M. Fekry

Chemistry Department, Faculty of Science, Cairo University, Giza-12613, Egypt.

\*E-mail: [Azzaghoneim@gmail.com](mailto:Azzaghoneim@gmail.com)

Received: 6 August 2012 / Accepted: 2 October 2012 / Published: 1 November 2012

---

Electrochemical techniques were used to characterize the corrosion behavior aluminum die casting alloy (A 383) in phosphoric acid without and with the individual addition of various halide anions (chloride  $\text{Cl}^-$ , bromide  $\text{Br}^-$ , iodide  $\text{I}^-$ ) or their oxyhalide ions of chlorate  $\text{ClO}_3^-$ , bromate  $\text{BrO}_3^-$  and iodate  $\text{IO}_3^-$ . The electrochemical impedance spectroscopy (EIS) and potentiodynamic polarization measurements indicate that the solution of 0.5 M  $\text{H}_3\text{PO}_4$  containing iodide ions is the most effective solution towards protective film formation with an inhibition efficiency (IE%) reaches to 88.9 %. However, the bromide ions have the most aggressive nature among the halides and oxyhalide ions as indicated from its higher corrosion current density  $i_{\text{corr}}$  value. The results were confirmed by surface examination via scanning electron microscope.

---

**Keywords:**

### 1. INTRODUCTION

Studies of the corrosion and stability of aluminum and its alloys are still of considerable interest because of their technological importance and industrial applications, especially in automobiles, aviation, household appliances, containers and electronic devices [1, 2]. Although pure Al is too soft to be used as a heavy duty material for large structures, high strength Al alloys can be produced by addition of appropriate alloying elements, such as Cu, Mg and Zn. The alloying elements and additives can generally influence the corrosion resistance of aluminum by forming mixed oxides that have compatible structures [3, 4]. Silicon (Si) is unquestionably the most important single alloying ingredient in the vast majority of aluminum casting alloys. Silicon is primarily responsible for so-called "good castability"; i.e. the ability to readily fill dies and to solidify castings with no hot tearing or hot cracking issues. Silicon is a very hard phase, thus it contributes significantly to an alloy's wear resistance, it combines with other elements to improve an alloy's strength and to make alloys heat

treatable. Al–Si alloys have been increasingly employed in the automotive industry, owing to their good castability, low thermal expansion coefficient and excellent mechanical properties [5, 6]. Aluminum die casting alloys are lightweight, offer good corrosion resistance, ease of casting, good mechanical properties and dimensional stability. Although a variety of aluminum alloys can be die cast from primary or recycled metal, most designers select A383 as one of the standard alloys, it provides better die filling but with a moderate sacrifice in mechanical properties such as toughness.

The application of aluminum and its alloys are often possible because of the natural tendency of aluminum to form a passivating oxide layer. However, in aggressive media, the passivating layer can be destroyed, and corrosive attack can take place. The protection of aluminum and its oxide films against the corrosive action of chloride ions have been extensively investigated [7-11].

S.S. Abdel Rehim et al [12] studied the corrosion behavior of pure Al, (Al + 6%Cu) and (Al+ 6%Si) alloys in  $\text{Na}_2\text{SO}_4$  solutions in the absence and presence of NaCl, NaBr and NaI. The corrosion resistance of the three Al alloys increases in the order  $\text{Al} < (\text{Al} + 6\% \text{Cu}) < (\text{Al} + 6\% \text{Si})$ . The results obtained showed that the addition of the halide ions increases the corrosion rates of the Al samples, and the aggressiveness of the halide ions towards the corrosion of Al and its two alloys increases in the order:  $\text{I}^- < \text{Br}^- < \text{Cl}^-$ . The breakdown of the passivating oxide films on Al and its alloys, by aggressive anions such as halides at sufficiently positive anodic potentials is

Frequently responsible for the failure of Al and its alloys in aqueous halide solutions, because it usually leads to severe pitting of the underlying metal. Pitting corrosion has been studied for several decades by many researchers and detailed information is available [13-16]. Similarly, the addition of certain inorganic oxysalts has a considerable effect on the corrosion performance of different metals and alloys [17-20]. Various attempts have been made to study the influence of different ions in solution on the electrochemical, inhibiting or enhancing pitting corrosion of Al and its alloys [21-24].

Phosphoric acid ( $\text{H}_3\text{PO}_4$ ) is a major industrial chemical, Electronics industry uses  $\text{H}_3\text{PO}_4$  in the preparation of semiconductors and printed circuit boards. Pure  $\text{H}_3\text{PO}_4$  is used in the food industry. It is also used in water treatment and to remove mineral deposits from process equipment and boilers. It acts as a binder for aluminum refractories. Phosphoric acid is widely used for acid cleaning and electropolishing of aluminum [25], but it still shows strong corrosiveness on aluminum and its alloys. Therefore, it is necessary to seek inhibitors for the corrosion of aluminum in  $\text{H}_3\text{PO}_4$ . The protection of metals against corrosion by  $\text{H}_3\text{PO}_4$  has been the subject of much study since it has been used in many industrial processes especially in fertilizer production [26, 27]. In our previous study [28] on A383 alloy, it was investigated that  $\text{K}_2\text{CrO}_4$  acts as a good corrosion inhibitor for the Al-Si alloy in  $\text{H}_3\text{PO}_4$  solution.

Accordingly, the purpose of the present work assumes great importance as it examines and assesses the influence of the various halide anions ( $\text{Cl}^-$ ,  $\text{Br}^-$ ,  $\text{I}^-$ ) in addition to their oxyanions including chlorate ( $\text{ClO}_3^-$ ), bromate ( $\text{BrO}_3^-$ ) and iodate ( $\text{IO}_3^-$ ) on the electrochemical behavior of aluminum die casting alloy (A383) in naturally aerated 0.5M  $\text{H}_3\text{PO}_4$  solutions using electrochemical techniques and surface examination.

## 2. EXPERIMENTAL

The working electrode is the aluminum die casting alloy (A383) rod with its cross-sectional area of  $0.785\text{cm}^2$ . The chemical composition of the alloy, as given by the supplier, is listed in Table 1.

**Table 1.** The chemical composition of A383 wt%

Al	Si	Zn	Cu	Fe	Mn	Mg	Sn	Ni	Cr	Pb	Na	Ti
79.952	10.614	2.91	2.52	0.918	0.21	0.057	0.052	0.05	0.069	0.052	0.041	0.38

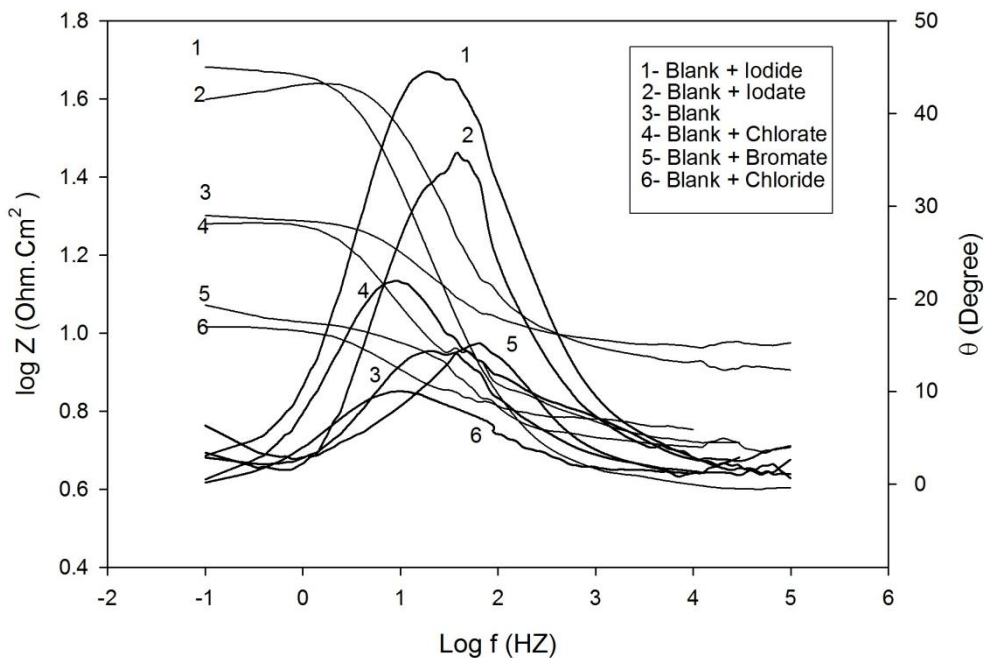
The test aqueous solutions contained 0.5M  $\text{H}_3\text{PO}_4$  (BDH) and potassium salts of chloride, bromide and iodide. The inorganic oxyanions were prepared from the potassium salts of bromate ( $\text{BrO}_3^-$ ), chlorate ( $\text{ClO}_3^-$ ) and iodate ( $\text{IO}_3^-$ ), Triple distilled water was used for preparing all solutions. In all measurements, mechanically polished electrode was used. Polishing was affected using successively finer grade of emery papers (600-1200 grade). Polarization and electrochemical impedance spectroscopy (EIS) measurements were carried out using the electrochemical workstation IM6e Zahner-electrik GmbH, Meßtechnik, Kronach, Germany. The excitation AC signal had amplitude of 10 mV peak to peak in a frequency domain from 0.1 Hz to 100 kHz. The EIS was recorded after reading a steady state open-circuit potential. The scanning was carried out at a rate  $30\text{mVmin}^{-1}$  over the potential range from  $-1500$  to  $+1000$  mV vs. saturated calomel electrode (SCE). Prior to the potential sweep, the electrode was left under open-circuit in the respective solution for  $\sim 2$  hours until a steady free corrosion potential was recorded. Corrosion current density,  $i_{\text{corr}}$ , which is equivalent to the corrosion rate, is given by the intersection of the Tafel lines extrapolation. Because of the presence of a degree of nonlinearity in the Tafel slope part of the obtained polarization curves, the Tafel constants were calculated as a slope of the points after  $E_{\text{corr}}$  by  $\pm 50$  mV using a computer least-squares analysis.  $I_{\text{corr}}$  were determined by the intersection of the cathodic Tafel line with the open-circuit potential. For surface examination, the electron microscope used is JEOL-JEM-100s type with magnification of 100x.

## 3. RESULTS AND DISCUSSION

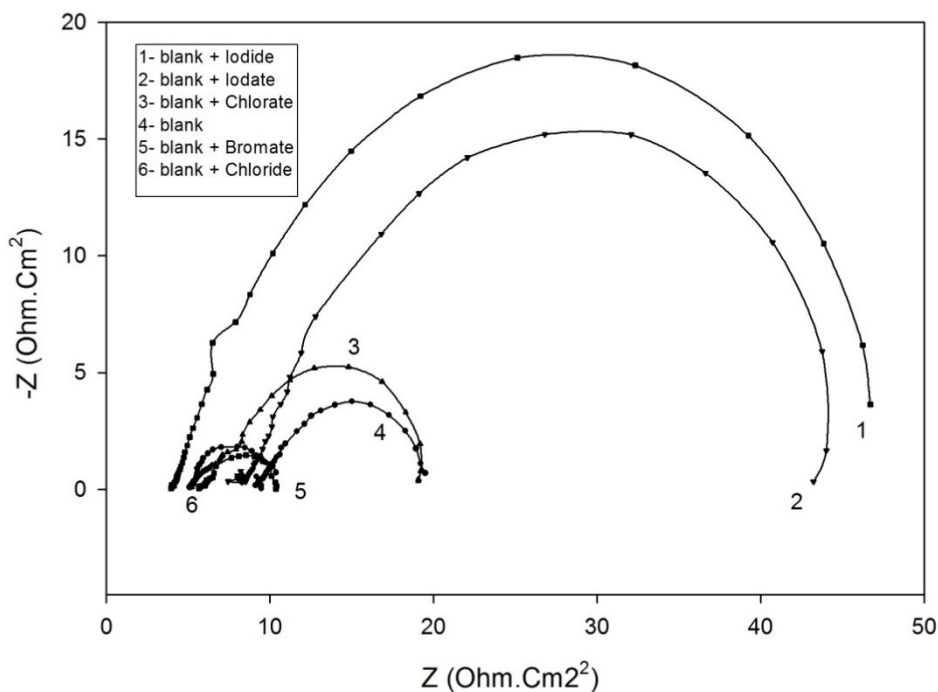
### 3.1. Electrochemical impedance measurements

#### 3.1.1. Effect of anion type

Electrochemical impedance (EIS) is one of the most powerful methods available in electrochemistry today. It can provide information on reaction parameters, corrosion mechanism and the action of compounds which influence the process. For corroding system, the objective of ac impedance is to model the corrosion process in terms of circuit elements, in order to be able to make conclusions about the characteristics of the corrosion process and its mechanism.



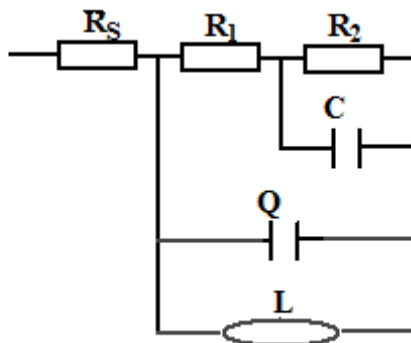
**Figure 1 (a).** Bode plots of A383 in 0.5 M H<sub>3</sub>PO<sub>4</sub> without and with different anions



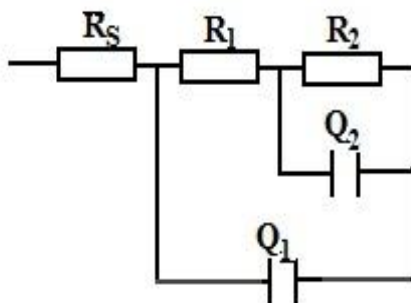
**Figure 1 (b).** Nyquist plots of A383 in 0.5 M H<sub>3</sub>PO<sub>4</sub> without and with different anions

Figure 1a,b represents the EIS data as Bode and Nyquist plots for the A383 alloy after 2 h immersion in 0.5 M H<sub>3</sub>PO<sub>4</sub> solution without and with the individual addition of 0.1 M halide ions, Cl<sup>-</sup>, Br<sup>-</sup>, I<sup>-</sup> or the addition of inorganic oxyhalide ions including chlorate (ClO<sub>3</sub><sup>-</sup>), bromate (BrO<sub>3</sub><sup>-</sup>) and Iodate ( IO<sub>3</sub><sup>-</sup>). It can be seen from the Bode format (Fig. 1a) that these diagrams show resistive regions at high and low frequencies and capacitive contribution at intermediate frequencies. The impedance

( $|Z|$ ) as well as the phase shift  $\theta$  for Al alloy are clearly found to depend on the nature of the ionic species prevailing in solution. The Nyquist plots (Fig. 1b), however, are characterized by well defined semicircles at high and medium frequency regions, the loop dimensions depend on the anion type. The impedance data were simulated to the appropriate equivalent circuit; this is the simulation that gives a reasonable fit using the minimum amount of circuit component.



**Figure 2 (a).** Equivalent circuit model representing 2 time constants for an electrode/electrolyte solution interface for blank, blank + KI



**Figure 2 (b).** Equivalent circuit model representing 2 time constants for an electrode/electrolyte solution interface for blank + ( $\text{Cl}^-$ ,  $\text{Br}^-$ ,  $\text{ClO}_3^-$ ,  $\text{BrO}_3^-$  and  $\text{IO}_3^-$ )

The proposed equivalent circuit manifested in Fig. 2(a), is used to analyze the impedance spectra of A383 in  $\text{H}_3\text{PO}_4$  solution without and with iodide ions. The model includes the solution resistance  $R_s$ , in a series combination of two resistances,  $R_1$  and  $R_2$ , which are in parallel with each of inductance,  $L$ , capacitance,  $C$  and the constant phase element,  $Q$ . Contribution to the total impedance at intermediate frequencies comes mainly from inductive component in parallel. The inductive loop is explained by the occurrence of adsorbed intermediate on the surface. Therefore, adsorbed intermediate species such as  $\text{Al}^+$  ads and  $\text{Al}^{3+}$  ads might be involved in Al dissolution process [29]. On the other hand, Iodide ions are usually characterized by strong adsorbability on the Al surface [25].

The inductor arise from adsorption effects could be defined as ( $L = R\tau$ ) where  $\tau$  is the relaxation time for adsorption on electrode surface. The low frequency locus displays the characteristics of parallel RC circuit. This circuit includes another constant phase element ( $Q$ ) which is placed in parallel

to  $R_1$  and  $R_2$ . The CPE is used in this model to compensate for nonhomogeneity in the system and is defined by two values,  $Q$  and  $\alpha$ . In order to understand the physical significance of each element of the electronic equivalent circuit, it can be considered that  $R_s$  corresponds to the solution resistance;  $R_1$  and  $R_2$  correspond to the polarization resistance of the surface of the samples and oxide film formations, respectively. The  $C$  and  $Q$  correspond to the capacitances of the experimentally examined samples and their oxide layer formation, respectively. The impedance of CPE is representing by [30]:

$$Z_{CPE} = Q^{-1} (i \omega)^{-\alpha} \quad (1)$$

where  $i = (-1)^{1/2}$ ,  $\omega$  is frequency in  $\text{rad s}^{-1}$ ,  $\omega = 2\pi f$  and  $f$  is the frequency in Hz. If  $\alpha$  equals one, the impedance of CPE is identical to that of a capacitor,  $Z_c = (i\omega C)^{-\alpha}$ , and in this case  $Q$  gives a pure capacitance ( $C$ ). Computer fitting of the spectrum allows evolution of the elements of the circuit analogue. The aim of the fitting procedure is to find those values of the parameters which best describe the data, i.e., the fitting model must be consistent with the experimental data.

Fig 2 (b) represents the equivalent circuit for the other anions and oxyanions in the same 0.5 M  $\text{H}_3\text{PO}_4$  solutions, this model consists only of two parallel combinations  $R_1Q_1$  and  $R_2Q_2$  in addition to the solution resistance  $R_s$  without the inductance  $L$ .

Analysis of the experimental spectra was made by best fitting to the corresponding equivalent circuit using Thales software provided with the workstation where the dispersion formula suitable to each model was used. In all cases, good conformity between theoretical and experimental was obtained for the whole frequency range with an average error of 5%. The experimental values were correlated to the theoretical impedance parameters of the equivalent model. The fit results of Nyquist plots and Bode plots for A383 after 2 h immersion in 0.5M  $\text{H}_3\text{PO}_4$  containing different halide and oxyhalide ions were presented in Tables 2, However, the results for the 2h immersion in the blank ( $\text{H}_3\text{PO}_4$ ) and in  $\text{H}_3\text{PO}_4$  containing iodide ions are found in Table 3.

**Table 2.** Equivalent circuit parameters of A 383 in 0.5 M  $\text{H}_3\text{PO}_4$  solution with 0.1 M different anions after 2 h immersion.

Anion	$R_1$ $\Omega \text{ cm}^2$	$Q_1$ $\mu\text{F cm}^{-2}$	$\alpha$ m	$R_2$ $\Omega \text{ cm}^2$	$Q_2$ $\mu\text{F cm}^{-2}$	$\alpha$ m	$R_s$ $\Omega$
$\text{IO}_3^-$	23.79	235.91	0.63	18.45	154.52	0.86	11.02
$\text{ClO}_3^-$	15.93	261.65	0.30	6.06	178.98	0.64	6.98
$\text{BrO}_3^-$	10.83	388.66	0.45	3.09	217.58	0.70	6.46
$\text{Cl}^-$	8.39	506.11	0.50	2.25	246.75	0.71	7.49
$\text{Br}^-$	0.103	703.21	0.43	0.032	416.52	0.7	3.29

The data and the figures indicate that the total resistance ( $R_T = R_1 + R_2$ ) of the surface film likely represents the corrosion resistance of the alloy and is inversely proportional to the corrosion rate, have the higher values in iodide containing phosphoric acid compared to the other halide and

oxyhalide ions, which could be attributed to the increase in the adsorbed amount of this anion on the electrode surface.

**Table 3.** Equivalent circuit parameters of A 383 in 0.5 M H<sub>3</sub>PO<sub>4</sub> solution without and with 0.1 M KI at different immersion time.

Anion	Time	R <sub>1</sub>	C	R <sub>2</sub>	Q	α	L	R <sub>s</sub>
Blank	(h)	Ω cm <sup>2</sup>	μF cm <sup>-2</sup>	Ω cm <sup>2</sup>	μF cm <sup>-2</sup>	m	kH	Ω
	0.00	16.20	42.54	6.66	65.46	0.75	40.18	10.14
	0.25	15.13	47.51	5.83	67.59	0.73	30.11	8.01
	0.50	14.84	49.17	4.82	70.45	0.71	29.13	8.95
	1.0	13.36	49.55	5.15	69.04	0.77	31.09	10.17
	2.0	14.79	46.24	5.74	67.02	0.75	33.08	11.81
	3.0	15.97	44.71	6.87	65.64	0.77	40.91	8.26
	24	31.50	31.97	7.18	61.56	0.79	48.10	9.31
	96	42.06	27.39	10.17	56.17	0.80	60.30	19.77
Blank +I <sup>-</sup>	0.00	17.93	265.09	30.20	227.89	0.84	822	4.65
	0.25	26.38	226.87	33.99	172.35	0.84	824	5.52
	0.50	25.28	229.68	32.58	182.54	0.85	850	5.56
	1.0	22.72	246.37	30.85	192.48	0.83	1103	5.57
	2.0	28.85	216.94	34.62	149.55	0.85	2421	5.21
	3.0	30.60	182.29	36.35	127.51	0.84	4969	4.75
	24	36.16	167.51	37.91	118.59	0.81	6712	6.06
	96	46.82	141.78	39.23	98.47	0.84	8458	7.65

The data also shows that for the halide ions Cl<sup>-</sup>, Br<sup>-</sup>, I<sup>-</sup> the value of R<sub>T</sub> and θ<sub>max</sub> decrease in the order I<sup>-</sup> > Cl<sup>-</sup> > Br<sup>-</sup> which might reflect the relative stability of the spontaneous passive film formed on the alloy surface in those media during the open-circuit immersion for 2h. This trend is most likely a result of an increase of surface film capacitance. This behavior assumes a higher rate of film formation in the solution of iodide compared to the chloride and bromide during the spontaneous growth process, suggesting that I<sup>-</sup> ion is more strongly adsorbed than either Cl<sup>-</sup> or Br<sup>-</sup> ions. It is undoubtedly due to an increase in the amount of specifically adsorbed iodide ions on the weak parts of the oxide covered alloy surface.

The same sequence was previously reported for zirconium electrode in halide solutions [31]. It was also investigated [32] that at potential values close to the corrosion potential I<sup>-</sup> ion could be adsorbed at the oxide covered Zr electrode with further formation of zirconium-iodide species. Hence, iodide can thus be considered as inhibiting anion for the A 383 corrosion where it imparts superior passivation to the alloy surface. On the other hand, iodate (IO<sub>3</sub><sup>-</sup>) has been reported to act as effective inhibitor for copper dissolution in acidic environments [18] and as corrosion inhibitor for (Ti-6Al-4V) alloy in H<sub>2</sub>SO<sub>4</sub>, HCl solutions [19]. Furthermore, iodate anion has been tested to exhibits induced passivation of AZ91D magnesium alloy in phosphate solution [17]. Accordingly, in this study, for the

three oxyhalogens, iodate solution shows the higher resistance to corrosion which is next to the iodide ion.

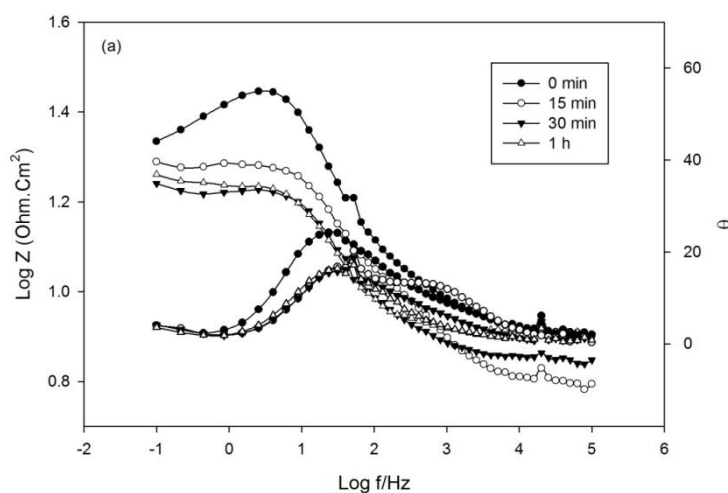
A plausible mechanism for the inhibition by oxyanions involves reduction of the anions themselves, depending on their nature, oxide formation and surface passivation are promoted [33]. In such cases the passive films become more stable and protect the metallic substrate from continuous corrosion. The redox reaction controls the chemistry of the film and is usually preceded by an adsorption step in which the inhibitive species adsorb on the active sites and then oxidation takes place [34]. In the presence of iodate anions, The significant decrease in corrosion rate may be for the reason that the adsorption of  $\text{IO}_3^-$  ions at flawed areas is the main factor for the inhibitive effect [17], as they facilitate the formation of aluminum oxide according to the following redox reactions,



On the other hand, the decrease in the inhibitive effect of chlorate and bromate solutions may be due to that the resultant chloride or bromide ions are harmful for the Al alloy as they enhance the preferential dissolution of Al from the grain matrix and participate in the corrosion attack of the surface. Hence, iodide and iodate medium are the most effective solutions toward protective film formation.

### 3.1.2 Effect of immersion time

EIS is a useful technique for long time tests, because they don't significantly disturb the system and it is possible to follow it over time. Thus in these experiments, the immersion of A383 alloy was carried out in 0.5 M  $\text{H}_3\text{PO}_4$  solution without and with the addition of 0.1 M KI up to 96h. Fig. 3(a,b) and 4(a,b) represent Bode plots in the blank and in blank containing 0.1 M KI solution respectively with time of immersion. It can be seen from the diagrams that the impedance  $|Z|$  as well as the phase shift  $\theta$  is clearly found to depend on immersion time. The equivalent circuit parameters of A383 in both solutions according to the proposed model (Fig. 2a) are presented in Table 3.



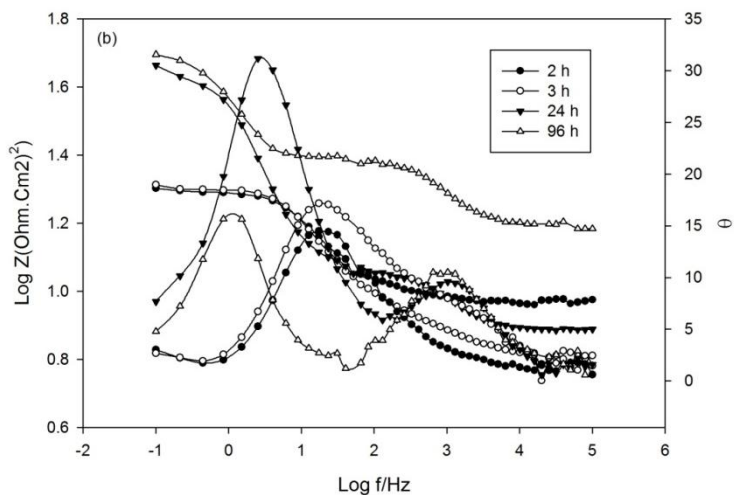


Figure 3. Bode plots of A383 in 0.5 M H<sub>3</sub>PO<sub>4</sub> at different immersion times

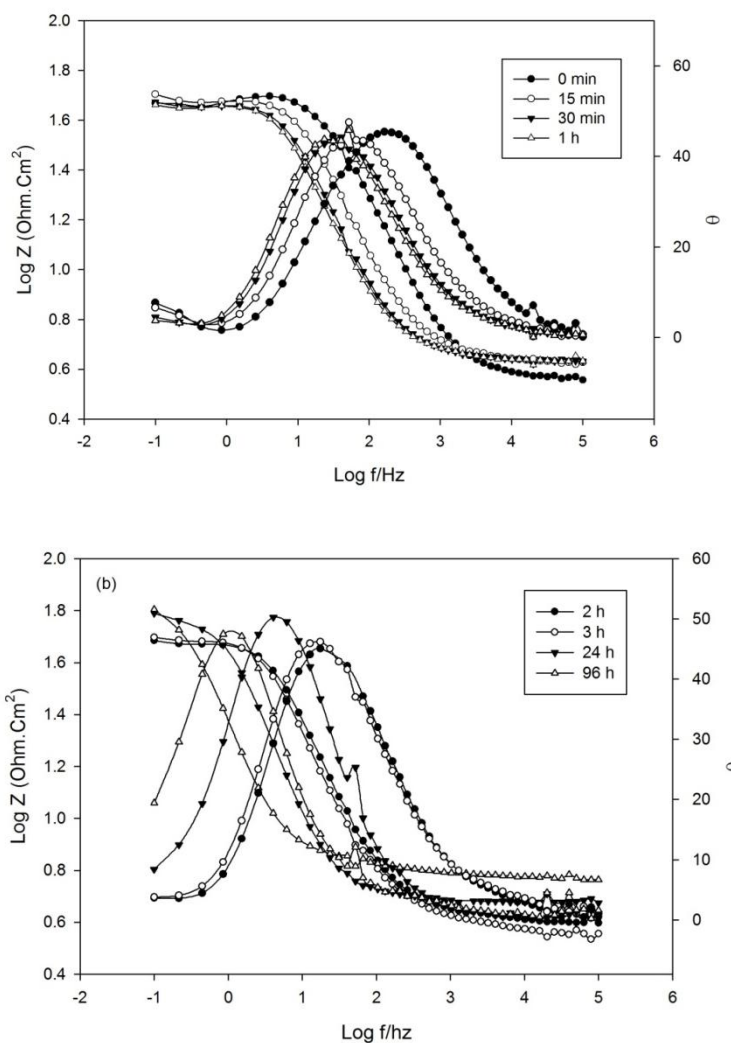
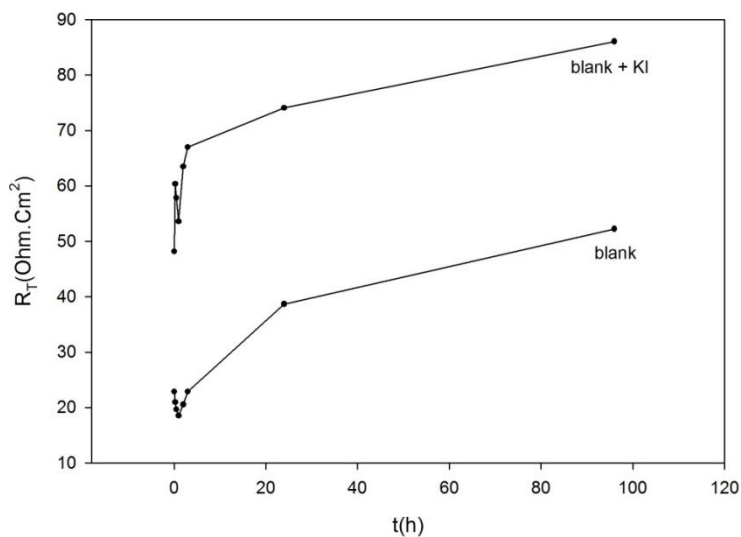


Figure 4. Bode plots of A383 in 0.5 M H<sub>3</sub>PO<sub>4</sub> with 0.1 M KI at different immersion times

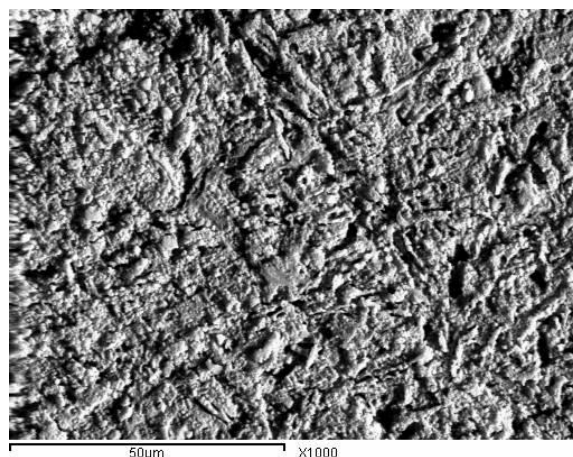
From the diagrams and EIS data in Table 3, it is obvious that the general trend in both solutions is that the resistance  $R_1$  and  $R_2$  of the surface film decrease slightly with time, while  $C$  and  $Q$  which are inversely proportional to the film thickness tend to increase during the first hour, then  $R_T$  starts to increase continuously with immersion time with concurrent decrease in each of  $C$  and  $Q$ .

Such behavior indicates the predominance of film dissolution process over the formation reaction during the first hour, above that film healing and thickening becomes effective.



**Figure 5.** Variation of the total resistance  $R_T$  of A383 with immersion time in 0.5 M  $H_3PO_4$  without and with 0.1 M KI

However, at any immersion time the value of  $R_T$  is always higher for A383 in 0.5 M  $H_3PO_4$  solution with 0.1 M KI as compared to A383 alloy in blank solution, suggesting that KI makes A383 alloy much more passive than the blank. Moreover, its higher  $\theta_{max}$  values compared to the blank indicate better dielectric properties due to the film formed in the iodide solution. Fig. 5 represents the variation of total resistance  $R_T$  with immersion time in 0.5 M  $H_3PO_4$  solution without and with 0.1 M KI.



(a)

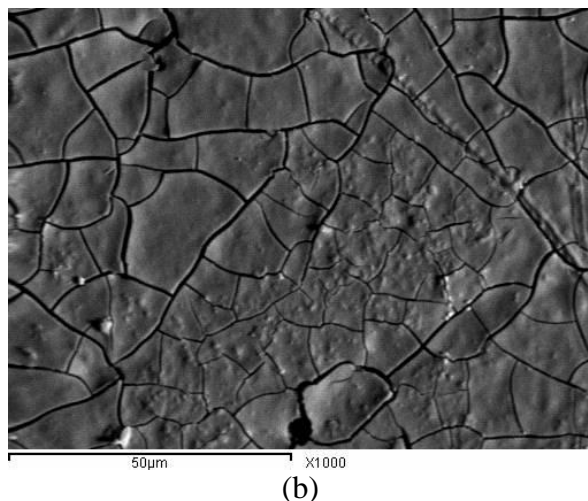


**Figure 6.** SEM images for tested electrode in 0.5 M  $\text{H}_3\text{PO}_4$  (blank) without (a), and with 0.1 M KI (b)

The results were further clarified by surface examination using scanning electron microscopy (SEM). Fig. 6 (a,b) represents the SEM micrographs for the tested electrode in 0.5 M blank solution (Fig. 6a) and in blank containing 0.1 M KI (Fig. 6b). The images show that a dense and smoother film is adsorbed on the alloy surface for the iodide containing solution than that for the blank.

### 3.2 Potentiodynamic Polarization Measurements

#### 3.2. Effect of anion type

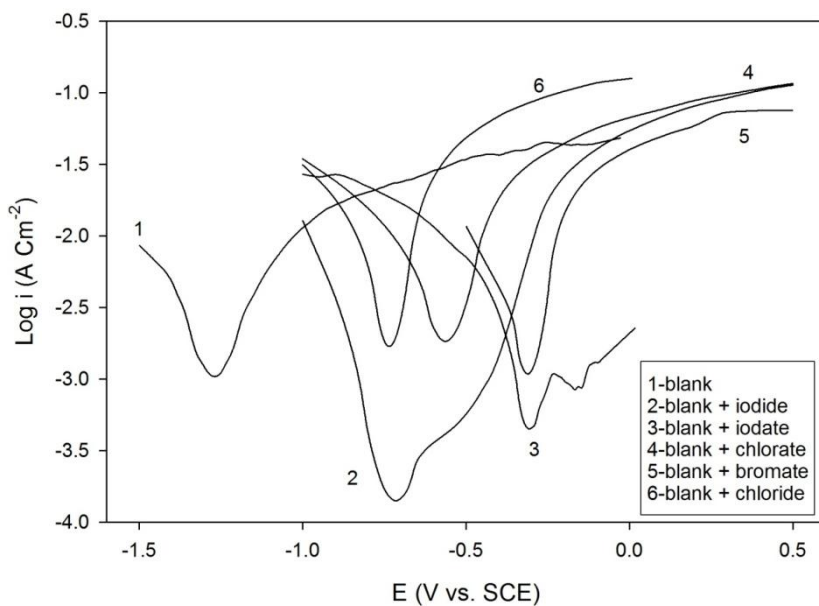


**Figure 7.** Potentiodynamic polarization curves of A383 in 0.5 M  $\text{H}_3\text{PO}_4$  without and with different anions

The potentiodynamic polarization behavior of A383 alloy was studied in 0.5 M H<sub>3</sub>PO<sub>4</sub> solution without and with individual addition 0.1 M solution of different anions including chloride Cl<sup>-</sup>, bromide Br<sup>-</sup>, iodide I<sup>-</sup> or their oxyanions, chlorate ClO<sub>3</sub><sup>-</sup>, bromate BrO<sub>3</sub><sup>-</sup> and iodate IO<sub>3</sub><sup>-</sup>.

Fig. 7 represents the potentiodynamic polarization curves at a scan rate of 1.0 mV s<sup>-1</sup>. Prior to the potential scan the electrode was left under open-circuit conditions in the respective solution for 2 h until a steady free corrosion potential value was recorded. Basically, in all solutions the alloy exhibit the same curve shape, no active-passive transition peak can discerned in the anodic trace, but a passivation plateau extending to a large domain of potential is observed. The corrosion potential (E<sub>corr</sub>) and corrosion current density (i<sub>corr</sub>) were calculated from the intersection of the anodic and cathodic Tafel lines extrapolation. The figure shows that the corrosion potential E<sub>corr</sub> is shifted towards more anodic potential in presence of the anions or oxyanions. The main electrochemical parameters of corrosion current density i<sub>corr</sub>, corrosion potential E<sub>corr</sub>, anodic Tafel slope β<sub>a</sub> and cathodic Tafel slope β<sub>c</sub> are presented in Table 4. The results indicate clearly that i<sub>corr</sub> depends on the anion nature, and there is a strong decrease in i<sub>corr</sub> in the blank containing KI solution. The results show that the properties of the Al alloy favors the formation of a passive film which confers great resistance to corrosion in KI medium leading to increase in R<sub>T</sub> value or decrease in corrosion rate.

**Table 4.** Corrosion parameters of A383 in 0.5 M H<sub>3</sub>PO<sub>4</sub> solution without and with 0.1 M different anions.

Anion	-E <sub>corr</sub> mV	i <sub>corr</sub> mAcm <sup>-2</sup>	-β <sub>c</sub> mV/dec	-β <sub>a</sub> mV/dec
Blank	1293	0.497	42	46
I <sup>-</sup>	749.7	0.055	26.2	98.3
IO <sub>3</sub> <sup>-</sup>	299.1	0.057	23.5	14.5
ClO <sub>3</sub> <sup>-</sup>	540.9	0.656	78.8	40.4
BrO <sub>3</sub> <sup>-</sup>	303.2	0.332	17.1	36
Cl <sup>-</sup>	722.8	0.807	70.3	44
Br <sup>-</sup>	549.9	431.8	43.6	79.7

Inspection of the Table reveals that bromide ions promote rapid corrosion of A383 more than in the other halide or oxyhalide ions. Such behavior reflects the harmful influence of Br<sup>-</sup> ions on the corrosion performance of the alloy in phosphoric acid. The anodic and cathodic scans exhibit higher polarization current reaches to 431.8 mAcm<sup>-2</sup>. The results are compatible well with those from EIS data.

On the other hand, it is evident from Table 4 that there is suppression in the corrosion rate in the aggressive H<sub>3</sub>PO<sub>4</sub> blank solution with respect to the solutions containing chloride, bromide ions or their oxyanions chlorate and bromate ions. These results may be due to the accumulation of the corrosion product in the film at the electrode / solution interface or through possible incorporation of PO<sub>4</sub><sup>3-</sup> anions into the lattice structure of the growing film [35].

A classification of anions into corrosion promoter and corrosion inhibitor is needed. Thus the inhibition efficiency (IE) of the two electrolytes containing blank + KI or  $\text{KIO}_3^-$  is calculated from the following equation [36]

$$IE\% = 1 - \frac{i_{inh}}{i_{corr}} \times 100 \quad (3)$$

where  $i_{corr}$  and  $i_{inh}$  are the uninhibited and inhibited corrosion current densities, respectively.

IE of 0.1M KI reaches up to 88.9 %, however for 0.1 M  $\text{KIO}_3^-$  is 88.5% which indicate that  $\text{I}^-$  and  $\text{IO}_3^-$  display a superior anticorrosion performance in  $\text{H}_3\text{PO}_4$  solution.

#### 4. CONCLUSIONS

The main points of this study are:

1. EIS measurements were carried out for the Al-Si alloy in 0.5 M  $\text{H}_3\text{PO}_4$  solution without and with the individual addition of 0.1 M solution of the halides,  $\text{Cl}^-$ ,  $\text{Br}^-$  and  $\text{I}^-$  or their oxyanions including  $\text{ClO}_3^-$ ,  $\text{BrO}_3^-$  and  $\text{IO}_3^-$ .
2. The presence of iodide or iodate ions in 0.5 M  $\text{H}_3\text{PO}_4$  solution increases the resistance  $R_T$  and decreases significantly the corrosion rate  $i_{corr}$ .
3.  $\text{Br}^-$  ions have the most aggressive nature among these halides or oxyhalides in which  $i_{corr}$  reaches a value of  $431.8 \text{ mAcm}^{-2}$ .
4. The inhibition efficiency for the adsorption of iodide and iodate ions is 88.9% and 88.5% respectively.
5. KI can be considered as useful for protecting A383 alloy against corrosion in  $\text{H}_3\text{PO}_4$  medium.

#### References

1. C. Vargel, *Corrosion of Aluminium*. Oxford, Elsevier, 2004.
2. B. Davó, J.J. Damborenea. *Electrochim. Acta*. 49(2004)4957.
3. H. Cordier, Ch. Dumont, W. Gruhl. *Aluminum*. 55, 777(1979).
4. DEJ Talbot, JDR Talbot. *Corrosion Science and Technology*: Taylor & Francis Group, 2007.
5. L. Lasa, J.M. Rodriguez-Ibabe. *Scripta Mater*. 46(2002)477.
6. L. Kyuhong, N.K. Yong. *J. Alloys Compd*. 461(2008)532
7. W.A. Badawy, F.M. Al-Kharafi, A.S. El-Azab. *Corros. Sci*. 41(1999)709.
8. Z. Grubac, R. Babic, M. Metikoš-Hukovic. *J. Appl. Electrochem*. 32(2002)431.
9. G.Y. Elewady, I.A. El-Said, A.S. Fouda. *Int. J. Electrochem. Sci*. 3(2008)177.
10. G.Y. Elewady, I.A. El-Said and A.S. Fouda. *Int. J. Electrochem. Sci*. 3(2008)644.
11. L. Vrsalovic\*, M. Kliškic and S. Gudic, *Int. J. Electrochem. Sci*. 4(2009)1568.
12. S.S. Abdel Rehim, H.H. Hassan, M.A. Amin *J. Appl. Surf. Sci*. 187 (2002)279.
13. F.M. Al-Kharafi, W.A. Badawy. *Corrosion*. 54(1998)377.
14. J.-D. Kim, S.-I. Pyun. *Electrochim. Acta*. 40(1995) 1863.

15. E. McCafferty. *J. Electrochem. Soc.* 137(1990) 3731.
16. A. Kolics, J.C. Polkinghorne, A. Wieckowski. *Electrochim. Acta.* 43(1998)3605.
17. F. El-Taib Heakal, A. M. Fekry, M. Z. Fatayerji *J. Appl. Electrochem.* 39(2009)1633.
18. Q. Luo. *Langmuir.* 16(2000)5154.
19. A. S. Mogoda, Y. A. Ahmad, W. A. Badawy. *Mat Corros.* 55(2004)449.
20. K. C. Emregul, A. A. Aksut. *Corros Sci* 45(2003)2415.
21. S.S. Abdel Rehim, H.H. Hassan, M.A. Amin, *Corros Sci.* 46(2004)1921.
22. A. Y. Musa, Abdul Amir H. Kadhum, Abu Bakar Mohamad, M. S. Takriff, E. P. Chee *Current Applied Physics.* 12(2012).325
23. L. Garrigues, N. Pebere, F. Dabosi. *Electrochim. Acta.* 41(1996)1209.
24. J. Zhao, G.S. Frankel, R.L. McCreery. *J. Electrochem. Soc.* 145(1998)2258.
25. M.A. Amin, Q. Mohsen, O.A. Hazzai. *Mater. Chem.Phys.* 114(2009)908.
26. E. Noor. *Corros. Sci.* 47(2005)33.
27. L. Wang. *Corros. Sci.* 48(2006)608.
28. M. A. Ameer, A. A. Ghoneim, A. M. Fekry. *Int. J. Electrochem. Sci.* 7(2012)4418,
29. M. Benabdellah, A. Aouniti, A. Dafali, B. Hammouti, M. Benkaddour, A. Yahyi, A. Ettouhami. *Appl. Surf. Sci.*252(2006)8341.
30. U. Rammelt, G. Reinhard. *Electrochim. Acta .* 35(1990)1045.
31. A. A. Ghoneim, *Materials and corrosion* 55(2004)617.
32. A. A. Ghoneim. H. M. Saleh, F. El-Taib Heakal, *monatsheft fur Chemie.* 129(1998)799.
33. CMABrett, IAR. Gomes, JPS. Martins. *J Appl Electrochem* 24(1994)1158.
34. S. Zein El-Abedin *J Appl Electrochem* 31(2001)711.
35. F. El-Taib Heakal, A. M. Fekry, M. Z. Fatayerji. *J. Appl. Electrochem* 39 (2009)583.
36. D. D. Macdonald. *Electrochim. Acta.* 35(1990)1509.